JOURNAL OF GEOPHYSICAL RESEARCH, VOL. 106, NO. D23, PAGES 32,283–32,294, DECEMBER 16, 2001

A one-dimensional simulation of the water vapor isotope HDO in the tropical stratosphere

Martin Ridal, Andreas Jonsson, Martin Werner, and Donal P. Murtagh[1]

Department of Meteorology, Stockholm University, Sweden

Abstract. An existing one-dimensional chemical model has been extended with dynamics and isotopic chemistry to simulate chemical production, vertical ascent, and diffusion of $H_2{}^{16}O$ and HDO in the tropical stratosphere. Less abundant isotopes of water vapor and methane have been added to the model's original chemical scheme. This has led to 11 additional compounds being considered, and the methane oxidation chain has been extended by 47 new reactions. The dynamical model includes vertical diffusion and a vertical ascent rate that varies throughout the year. The results of the model show values of the isotopic ratio that are expected from theoretical calculations. The δD values range from around $-550‰$ at the tropopause to about $-300‰$ at 1 hPa. The model simulations are also in agreement with the few existing measurements of δD in the stratosphere. An annual variation of the isotopic ratio at the tropopause will cause a wave pattern in the vertical profile similar to the "tape recorder effect" for water vapor. The size and shape of this annual variation is not clear, but simulations show that the effect it has on the resulting δD profile is significant.

1. Introduction

The general circulation of the stratosphere is rather well known although many details are still not fully understood. Water vapor is a very useful tool in studying many of these details due to its long chemical lifetime [e.g., *Holton*, 1984; *Brasseur and Solomon*, 1984]. The largest inputs of water vapor are believed to take place at the tropical tropopause. This area holds the lowest temperature an air parcel will experience on the way from the ground and up into the stratosphere. The tropopause will act as a "cold trap" where the water vapor freezes out and the crystals fall back into the troposphere, leaving very dry air in the lowest stratosphere. The tropopause temperature will thus have a strong influence on the amount of water vapor allowed to enter the stratosphere. The temperature in this region experiences a very distinct annual cycle, with higher temperature during northern summer and lower during winter. The amount of water vapor that enters the stratosphere will therefore also follow an annual cycle [*Mote et al.*, 1995, 1996].

Inside the stratosphere, water vapor is produced by methane oxidation. It is primarily OH and $O(^1D)$ that react with one methane molecule to produce two water molecules [e.g., *Brasseur and Solomon*, 1984; *Le Texier at al.*, 1988]. This causes the mixing ratio of water vapor to increase with altitude. Above 50 km, water molecules are destroyed by photolysis and the profile starts to decrease.

In the midlatitudes, planetary (and gravity) waves break in the upper stratosphere. The region was named the "surf zone" by *McIntyre and Palmer* [1984] for this reason. The net effect of the wave breaking is movement of air toward the poles. For continuity reasons, there will be an ascending motion in the tropical stratosphere. *Holton et al.* [1995] called the breaking waves "the extratropical pump." Water vapor that enters the stratosphere at the tropical tropopause will thus be transported upward. Since the tropical stratosphere is rather isolated and the input of water vapor follows a distinct annual cycle, the pattern of high and low amounts of water may be followed as it moves upward in time. This "tape recorder effect" was first discovered by *Mote et al.* [1995].

In the midlatitudes, there are also stratosphere to troposphere exchange (STE) events taking place. The exact mechanism causing this, as well as the amount and direction of transport, is not completely clear. Tropopause folds and cutoff lows have been mentioned as possible mechanisms [*Holton et al.*, 1995].

Apart from the main isotope of water, $H_2{}^{16}O$ (hereinafter referred to as H_2O), less abundant water vapor isotopes are also potential tracers of the stratospheric dynamics [e.g., *Kaye*, 1990; *Rinsland et al.*, 1991; *Moyer*

[1]Now at Chalmers University of Technology, Göteborg, Sweden.

Paper number 2000JD000268.
0148-0227/01/2000JD000268$09.00

et al., 1996]. They can be used in the same way as the main isotope, but also by looking at the isotopic ratio, i.e., the amount of heavy isotopes compared to the main isotope. The isotopic ratio would be especially useful to study when determining whether an air parcel has been formed inside the stratosphere from methane oxidation or if it is transported in from the troposphere (see section 2). This could give important information about STE in the tropical region but it could also be a way to obtain a better knowledge of STE at midlatitudes. The fact that the isotopic ratio of water vapor formed in the stratosphere is different from that of water entering from below also makes it possible to study the "age of air" and mixing between different regions of the stratosphere (subtropical barriers, polar vortex).

In this work, a one-dimensional model has been constructed to simulate the isotopic ratio of water vapor in the tropical stratosphere. The purpose of these simulations is to help our understanding of how the isotopic ratio changes with altitude. It is also part of the preparatory work for the Odin satellite (see a further discussion in section 6.3). The model is currently designed for simulations in the tropical region. The input of water vapor follows an annual cycle according to the tape recorder theory, with large injections during Northern Hemispheric summer and small injections during winter [*Mote et al.*, 1995, 1996]. A large-scale ascending motion transports the water vapor upward. The model domain is assumed to be entirely in the stratosphere with the tropopause fixed at 100 hPa, which is the lowest layer. It covers the altitude range 16-50 km (1-100 hPa) with a vertical resolution of 1 km. The annual variation of tropopause height has been ignored, but this will not significantly influence the results.

The original chemistry model includes 44 different molecules and 112 reactions. Thus far the included isotopic water vapor molecules are H_2O and HDO. When HDO was included in the model we had to add 11 more compounds with 1 H replaced by D. This leads to 47 new reactions in the methane oxidation chain. We have not included $H_2{}^{18}O$ in the model because its production is not yet completely understood. For example, the influence of the isotopic signature of O_3 in the middle and upper stratosphere, through oxidation of methane by $O(^1D)$, is not established.

Isotopic compositions of a measurement or model output is usually expressed using a delta notation. The isotopic ratio (for example, deuterium to hydrogen) of the sample of interest is related to a reference sample by

$$\delta D = \left(\frac{(D/H)_m - (D/H)_{ref}}{(D/H)_{ref}} \right) 1000. \qquad (1)$$

The unit is part per thousand and the reference ratio is usually taken from a standard water probe. The most widely used standard for reporting isotopic compositions of oxygen and hydrogen in natural samples is the Standard Mean Ocean Water (SMOW), first presented by *Craig* [1961].

The $(D/H)_m$ is the modeled (or measured) isotopic ratio of water vapor and calculated as

$$(D/H)_m = \frac{\kappa(HDO)}{2 \times \kappa(H_2O)}, \qquad (2)$$

where $\kappa(HDO)$ and $\kappa(H_2O)$ are the modeled mixing ratios. In this work we use for $(D/H)_{ref}$ the recommended SMOW value by *Hagemann et al.* [1970], which is $155.76 \times 10^{-6} \pm 0.05 \times 10^{-6}$.

2. Theory

The mechanisms that affect the isotopic ratio of water in an air parcel can be of a different nature. For example, the heavier water isotopes have a lower vapor pressure than the main isotope and are therefore enriched in the condensated phase. This effect is known as vapor pressure isotope effect (vpie) [*Jancso and van Hook*, 1974] and occurs both during evaporation and condensation of water. In general, the vpie is the dominating fractionation effect; however, an additional, kinetic fractionation effect exists, which is mainly important during evaporation processes [*Merlivat and Jouzel*, 1979]. This fractionation effect is related to the slightly lower diffusivity of the heavier water isotopes.

In the troposphere an air parcel can go through many phase changes and experience many different temperatures, especially in the tropics with its deep convective cells. Following the so-called Rayleigh fractionation, taking these fractionation processes and their temperature dependence into account [*Dansgaard*, 1964], the depletion of the heavier isotopes in water vapor would be very severe at the top of the troposphere. Expected δD values would be in the range of $-700‰$ to $-800‰$. However, these values do not show up in the measurements. The δD values reported in the literature are between $-500‰$ and $-600‰$ (e.g., *Ehhalt* [1974]; review by *Kaye* [1987], or *Smith* [1992]). *Smith* [1992] suggests that the reason for the lesser depletion is, what he calls, "ice lofting." The updrafts inside the convective clouds will carry ice particles upward from low altitudes, where the isotopic depletion is less. These ice particles can then detrain from the cloud at higher altitudes and evaporate, causing a higher isotopic ratio than expected.

The isotopic ratio of water vapor produced inside the stratosphere will be determined by the isotopic content of its sources. Since the only production of water vapor is through methane oxidation the amount of HDO will reflect the isotopic content of methane. The D/H ratio for methane is larger relative to that for water vapor and has a delta value of about $-50‰$ to $-100‰$ in the troposphere and lower stratosphere [e.g., *Rinsland et al.*, 1991; *Irion et al.*, 1996].

The relative amount of HDO in the total water content is therefore expected to increase with altitude in the stratosphere. At the tropopause it will be very low δD=$-500‰$ to $-600‰$, and at 50 km we expect a

delta value of about $-200‰$. It will not fully reflect the δD value of methane since there will still be some influence of the tropopause value.

3. Model Description

A one-dimensional dynamical model has been integrated with the MISU 1-D chemical model developed by Andreas Jonsson at the Department of Meteorology, Stockholm University. The production and loss from the chemistry is calculated between each dynamical time step. By decoupling the chemistry and the dynamics (advection and diffusion) the model can perform several chemical time steps during one dynamical time step. Only the species with a long chemical lifetime are then passed on to the dynamical model. These species are considered to be H_2O, CH_4, H_2, and N_2O.

To the original chemistry we have added those heavier isotopes of water vapor and methane which include one deuterium atom. The methane oxidation chain has therefore been extended with isotopic chemistry, including a number of new compounds and reactions. A few of these compounds are long lived and have been included in the dynamical model.

3.1. Chemistry

The chemical model is a one-dimensional model simulating stratospheric gas phase chemistry. The model includes a chemistry module, based on a chemical scheme by *Grooss* [1996], which contains 44 species, including oxygen compounds: O, $O(^1D)$, O_3, O_2; hydrogen compounds: H_2O, H_2, H, OH, HO_2, H_2O_2; nitrogen compounds: N_2, N_2O, N, NO, NO_2, NO_3, N_2O_5, HNO_3, HO_2NO_2; chlorine compounds: Cl, ClO, ClOO, Cl_2O_2, OClO, Cl_2, HCl, HOCl, $ClONO_2$, $ClNO_2$; bromine compounds: Br, BrO, BrCl, HBr, HOBr, $BrONO_2$; and methane and its oxidation products, including CO. Eighty-six gas phase reactions and 26 photolysis reactions are included for which the data are taken from *DeMore et al.* [1997].

The model is initialized by monthly (April) zonal mean profiles of temperature, H_2O, CH_4, NO, NO_2, and HCl measured by HALOE from 1992 to 1998. Other compounds are initialized by noon monthly mean profiles derived from a 10 year climatology calculated by the Canadian Middle Atmosphere Model (CMAM) [*de Grandpre et al.*, 1997].

Detailed radiation calculations in the UV and visible regions, including multiple scattering, are performed to calculate a photolysis rate look-up table. The chemical reaction scheme generates a system of stiff ordinary differential equations (ODE) of the type

$$\frac{dn_i}{dt} = P_i + L_i, \tag{3}$$

where n_i is the concentration of the ith compound. P_i and L_i are the production and loss rates derived from the chemical reactions in which n_i participates. For example, the ODE describing the concentration of HD is the following:

$$\frac{d[HD]}{dt} = K_8[D][HO_2] - K_{4a}[OH][HD] + K_{4b}[OH][HD] + J_3[CHDO], \tag{4}$$

where the coefficients K are chemical reaction rates, and J is a photolysis rate. The full ODE system is solved by using a quasi-constant step size variable order solver based on numerical differentiation formulas [*Shampine and Reichelt*, 1997]. Photolysis rates are updated at each time step.

A full diurnal cycle can be simulated with photolysis rates provided from the look-up table at each time step. To minimize the computational cost the chemical model is run at a constant solar zenith angle of 60°.

3.2. Isotopic Chemistry

When including the isotopes of water and methane in the oxidation chain, there are a number of new products and reactions that have to be included to complete the methane oxidation chain. The new compounds added to the chemical model are HDO, CH_3D, CH_2D, OD, HD, D, DCl, DO_2, CH_2DO_2, CH_2DOOH, CH_2DOH, CHDO. The initial profiles for HDO, CH_3D, and HD are set to match the δD values found in literature (see section 2). The other compounds are just set to 0.1% of the unsubstituted equivalent (e.g., for CHDO this would be 0.1% of CH_2O). These compounds have a relatively short chemical lifetime, so the initial profile does not effect the resulting profile.

The following new reactions were added to the model

(R_1)	HDO	+ $O(^1D)$	→ OH	+ OD
(R_{2a})	CH_3D	+ $O(^1D)$	→ CH_3	+ OD
(R_{2b})			→ CH_2D	+ OH
(R_{3a})	CH_3D	+ OH	→ CH_3	+ HDO
(R_{3b})			→ CH_2D	+ H_2O
(R_{4a})	HD	+ OH	→ HDO	+ H
(R_{4b})			→ H_2O	+ D
(R_5)	CH_4	+ OD	→ CH_3	+ HDO
(R_6)	OD	+ H_2	→ HDO	+ H
(R_7)	D	+ HO_2	→ HDO	+ O
(R_8)	D	+ HO_2	→ HD	+ O_2
(R_9)	D	+ HO_2	→ OD	+ OH
(R_{10})	H	+ DO_2	→ HDO	+ O
(R_{11})	H	+ DO_2	→ HD	+ O_2
(R_{12})	H	+ DO_2	→ OD	+ OH
(R_{13})	D	+ O_3	→ OD	+ O_2
(R_{14a})	CH_3D	+ Cl	→ CH_3	+ DCl
(R_{14b})			→ CH_2D	+ HCl

$$(R_{15})\quad CH_2DO_2 + HO_2 \rightarrow CH_2DOOH + O_2$$

$$(R_{16a})\quad CH_2DO_2 + NO \rightarrow CH_2O + NO_2 + D$$
$$(R_{16b})\quad \rightarrow CHDO + NO_2 + H$$

$$(R_{17a})\quad CH_2DO_2 + ClO \rightarrow CH_2O + DO_2 + Cl$$
$$(R_{17b})\quad \rightarrow CHDO + HO_2 + Cl$$

$$(R_{18a})\quad CH_2DO_2 + CH_3O_2 \rightarrow CHDO + CH_3OH + O_2$$
$$(R_{18b})\quad \rightarrow CH_2O + CH_2DOH + O_2$$

$$(R_{19})\quad CH_2DO_2 + CH_2DO_2 \rightarrow CHDO + CH_2DOH + O_2$$

$$(R_{20})\quad CH_2DOOH + OH \rightarrow CH_2DO_2 + H_2O$$

$$(R_{21a})\quad CH_2DOOH + OH \rightarrow CH_2O + OH + HDO$$
$$(R_{21b})\quad \rightarrow CHDO + OH + H_2O$$

$$(R_{22a})\quad CH_2DOOH + Cl \rightarrow CH_2O + OH + DCl$$
$$(R_{22b})\quad \rightarrow CHDO + OH + HCl$$

$$(R_{23})\quad DCl + OH \rightarrow HDO + Cl$$

$$(R_{24})\quad HCl + OD \rightarrow HDO + Cl$$

$$(R_{25})\quad CHDO + OH \rightarrow HDO + HCO$$

$$(R_{26})\quad CH_2O + OD \rightarrow HDO + HCO$$

$$(R_{27})\quad CHDO + Cl \rightarrow DCl + HCO$$

$$(R_{28a})\quad CH_2DOH + OH \rightarrow CH_2O + H + HDO$$
$$(R_{28b})\quad \rightarrow CHDO + H + H_2O$$

$$(R_{29a})\quad CH_2DOH + OH \rightarrow CH_2O + H + DCl$$
$$(R_{29b})\quad \rightarrow CHDO + H + HCl$$

We have not included reactions where both reactants contain 1 deuterium atom, for example, HD + OD, since the low amounts of both compounds will give an insignificant contribution to the respective products. In reactions (R_{25})-(R_{27}), as well as photolysis reaction (P_5) (section 3.2.2) we do not consider the possible formation of DCO. This compound has a very rapid conversion to form DO_2 that will result in the production of a HDO molecule.

3.2.1. Rate constants. The reaction rate constants, k_n, for the reactions above are taken from the Jet Propulsion Laboratory (JPL) catalog [*DeMore et al.*, 1997] where available. In most cases, however, they are set to the same value as for the corresponding isotopically unsubstituted reaction. In many of the reactions the deuterium can end up in two (or even three) different products. The different rate constants used and a motivation for why these are chosen are given below. Value n is the corresponding reaction number and the units for all are cm^3 $molecule^{-1}$ s^{-1}.

$k_1 = 2.2 \times 10^{-10}$ same as for the unsubstituted reaction; according to *Kaye* [1987] this reaction is about 1% slower;

$k_{2a} = 0.38 \times 10^{-10}$ 25% of the unsubstituted reaction; there is one chance of four that the D will leave the CH_3D; very little isotopic effect according to *Kaye* [1987];

$k_{2b} = 1.13 \times 10^{-10}$ 75% of the unsubstituted reaction; three chances of four that the D will stay;

$k_{3a} = 0.88 \times 10^{-12}$ 25% of the rate constant in JPL (3.51×10^{-12}); same motivation as for k_2;

$k_{3b} = 2.63 \times 10^{-12}$ 75% of the rate constant in JPL;

$k_{4a} = 2.5 \times 10^{-12}$ rate constant 5×10^{-12} from JPL; 50% for this branch;

$k_{4b} = 2.5 \times 10^{-12}$ and 50% for this;

$k_5 = 2.45 \times 10^{-12}$ same value as for the unsubstituted reaction;

$k_6 = 5.5 \times 10^{-12}$ same value as for the unsubstituted reaction; only these products are considered since it is not very likely that the OD will break to form H_2O + D;

$k_7 = 1.62 \times 10^{-12}$ same value as for the unsubstituted reaction;

$k_8 = 7.29 \times 10^{-12}$ same value as for the unsubstituted reaction;

$k_9 = 1.4 \times 10^{-10}$ same value as for the unsubstituted reaction;

$k_{10} = 1.62 \times 10^{-12}$ same value as for the unsubstituted reaction;

$k_{11} = 7.29 \times 10^{-12}$ same value as for the unsubstituted reaction;

$k_{12} = 1.4 \times 10^{-10}$ same value as for the unsubstituted reaction;

$k_{13} = 7.05 \times 10^{-11}$ same value as for the unsubstituted reaction;

$k_{14a} = 0.21 \times 10^{-11}$ 25% of the value given in JPL for this reaction; this value is only for T=298 K, so we assume the same temperature dependence as for the unsubstituted reaction;

$k_{14b} = 0.62 \times 10^{-11}$ 75% of the value given in JPL;

$k_{15} = 3.8 \times 10^{-13}$ same value as for the unsubstituted reaction;

$k_{16a} = 1.0 \times 10^{-12}$ one third of the unsubstituted reaction; same motivation as for k_2, but in this case, there are three possible choices;

$k_{16b} = 2.0 \times 10^{-12}$ two thirds of the unsubstituted reaction;

$k_{17a} = 0.55 \times 10^{-12}$ one third of the unsubstituted reaction; same motivation as for k_{16};

$k_{17b} = 1.10 \times 10^{-12}$ two thirds of the unsubstituted reaction; same motivation as for k_{16};

$k_{18a} = 1.25 \times 10^{-13}$ 50% of the unsubstituted reaction; in this case it is hard to determine the possible ways the D can go; for simplicity we use 50% for both this branch;

$k_{18b} = 1.25 \times 10^{-13}$ and 50% for this branch;

$k_{19} = 2.5 \times 10^{-13}$ same value as for the unsubstituted reaction;

$k_{20} = 2.66 \times 10^{-12}$ same value as for the unsubstituted reaction; the products CH_3O_2 + HDO are not included since it is most probable that the O-OH bond will break due to the polarization of the molecule;

$k_{21a} = 0.38 \times 10^{-12}$ one third of the unsubstituted reaction; we do not consider the formation of OD since it is very unlikely that the OH will split up; the other two branches are considered in the same way as k_{16};

$k_{21b} = 0.76 \times 10^{-12}$ two thirds of the unsubstituted reaction;

$k_{22a} = 2.63 \times 10^{-11}$ one third of the unsubstituted reaction; same motivation as for k_{21};

$k_{22b} = 5.27 \times 10^{-11}$ two thirds of the unsubstituted reaction;

$k_{23} = 2.6 \times 10^{-12}$ same value as for the unsubstituted reaction;

$k_{24} = 2.6 \times 10^{-12}$ same value as for the unsubstituted reaction;

$k_{25} = 1.0 \times 10^{-11}$ same value as for the unsubstituted reaction; in this reaction, and the two following, we do not consider the possible formation of DCO (see end of section 3.2);

$k_{26} = 1.0 \times 10^{-11}$ same value as for the unsubstituted reaction (see comment for k_{25});

$k_{27} = 8.1 \times 10^{-11}$ same value as for the unsubstituted reaction (see comment for k_{25});

$k_{28a} = 2.30 \times 10^{-12}$ one third of the unsubstituted reaction (see comment for k_{21});

$k_{28b} = 4.60 \times 10^{-12}$ two thirds of the unsubstituted reaction;

$k_{29a} = 1.80 \times 10^{-11}$ one third of the unsubstituted reaction (see comment for k_{21});

$k_{29b} = 3.60 \times 10^{-11}$ two thirds of the unsubstituted reaction.

3.2.2. Photochemical reactions. Four of the new compounds, HDO, DCl, CHDO, and CH_2DOOH, are also destroyed by photolysis. The photolysis rates for the new reactions given below are set to be the same as for the corresponding unsubstituted reaction. For (P_1) we assume that the two branches are equally possible and use half the value of the photolysis rate in each reaction. For (P_5) we assume one third of the photolysis rate for branch a and two thirds for branch b (see comment for k_{16}). In (P_5) we do not consider the formation of OD (see comment for k_{21}). The reactions added to the photochemical reaction scheme are

(P_{1a})	HDO	+ hν	$\rightarrow$ OH	+ D
(P_{1b})			$\rightarrow$ OD	+ H
(P_2)	DCl	+ hν	$\rightarrow$ Cl	+ D
(P_3)	CHDO	+ hν	$\rightarrow$ CO	+ HD
(P_4)			$\rightarrow$ HCO	+ D
(P_{5a})	CH_2DOOH	+ hν	$\rightarrow$ CH_2O	+ OH + D
(P_{5b})			$\rightarrow$ CHDO	+ OH + H

3.3. Dynamical Model

The dynamical motions in the model includes the large-scale upward advection as well as the vertical diffusion, parameterized by the eddy diffusion approximation. The time dependence of the mixing ratio in each layer is calculated according to

$$\frac{\partial M}{\partial t} + w\frac{\partial M}{\partial z} + \frac{\partial}{\partial z}\left(-K_z N \frac{\partial M}{\partial z}\right) + P - L = 0, \quad (5)$$

where M is the mixing ratio, for example, H_2O in parts per million by volume (ppmv). Value w is the vertical velocity in m/s, and the vertical diffusion coefficient is given by K_z (m^2/s). N is the density of air in molecules/cm^3. P and L denotes chemical production and loss rates, respectively (obtained from the chemical model).

A standard leapfrog scheme is used to solve Equation (5). The length of the time step is currently set to 5 days but can be varied.

The vertical ascent rate, given by w (m/s), is allowed to vary throughout the year. The annual cycle of w follows calculations by *Mote et al.* [1996] who found that the vertical ascent in the tropical region is stronger during the northern winter season. In the model the vertical velocity varies as a sine wave around a mean value of 0.3×10^{-3} m/s with a maximum of 0.42×10^{-3} m/s during the winter and a minimum value of 0.18×10^{-3} m/s in the summer season.

The vertical motions due to diffusion are calculated using a diffusion coefficient, K_z. We tried different approaches for K_z, given by *Brasseur and Solomon* [1984], *Owens et al.* [1985], and *Brühl and Crutzen* [1988], to

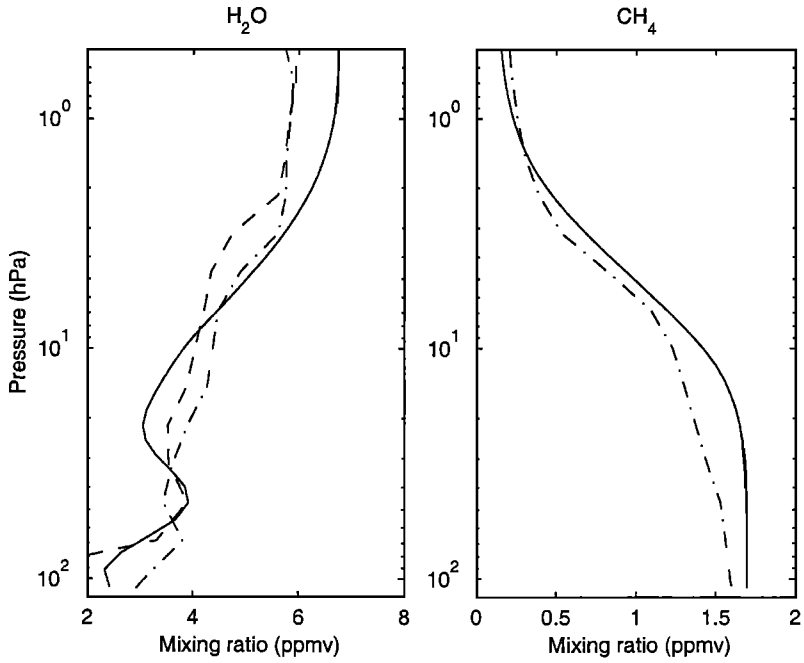

Figure 1. Solid lines are water vapor (left) and methane (right) from April simulated by the 1-D model. The dashed line is tropical (-10° to 10°) measurements by the MLS instrument from April 1993 and the dotted-dashed lines are the same by the HALOE instrument, both on the UARS satellite.

find a coefficient that is sufficiently strong but does not destroy the tape recorder pattern. The coefficient used in this work is based upon values from *Owens et al.* [1985] and calculated according to

$$K_z = 1 \times 10^{-3} \exp(z/11). \quad (6)$$

Since we also have transport by advection included, the diffusion coefficient here is a little less than the values given by *Owens et al.* [1985] where the only vertical transport was due to vertical diffusion.

3.4. Boundary Conditions

Inflow at the lower boundary, simulating input from the troposphere, is prescribed for the long-lived species, for example, water vapor and methane, and their isotopic equivalents. A virtual layer is created below the lowest model layer in which the mixing ratios for these compounds are prescribed. All mixing ratios except water vapor are constant.

According to the "stratospheric tape recorder" theory [*Mote et al.*, 1995] the input of water vapor in to the tropical lower stratosphere follows a very pronounced annual cycle. To simulate the varying inflow, the prescribed H_2O mixing ratio in the virtual layer is allowed to vary in time. In the model, the main water vapor isotope follows a sine wave around a mean value of 3.5 ppmv with an amplitude that is one third of this value. The lowest values are found during Northern Hemisphere winter and the highest during summer.

The deuterated water vapor (HDO) varies similarly through time but around the mean value 0.45×10^{-3} ppmv. This value was chosen to set the mean value of $\delta D = -580‰$. Measurements of HDO in the upper troposphere show a variety of different δD values (e.g., *Ehhalt* [1974], review by *Kaye* [1987], and *Smith* [1992]). We found that this is a good estimate of a mean value of measurements at the top of the tropopause (see section 2).

An annual variation of the input δD value can also be simulated by varying the relative amplitude of the H_2O and HDO cycles. If the relative amplitude of the HDO input cycle is the same as that of H_2O (one third of the respective mean value), the δD value will be constant in time. If the relative HDO amplitude is higher, we will create a stronger depletion during winter and less depletion during the summer season. The opposite effect is created if the relative amplitude of the isotope input wave is lower than that of H_2O.

How the annual cycle of the delta value for water vapor should be chosen is not known at the moment. In section 6.2 we will discuss how the different scenarios will affect the vertical profile of δD.

The CH_3D mixing ratio at the tropopause is assumed to be 9.9×10^{-4} ppmv, while the unsubstituted methane has a mixing ratio of 1.7 ppmv. This corresponds to a δD value for methane of $-65‰$. This value is in the range of what has been observed around the tropopause [e.g., *Rinsland et al.*, 1991; *Irion et al.*, 1996].

At the upper boundary of the model we assume that the compounds are allowed to be transported out of

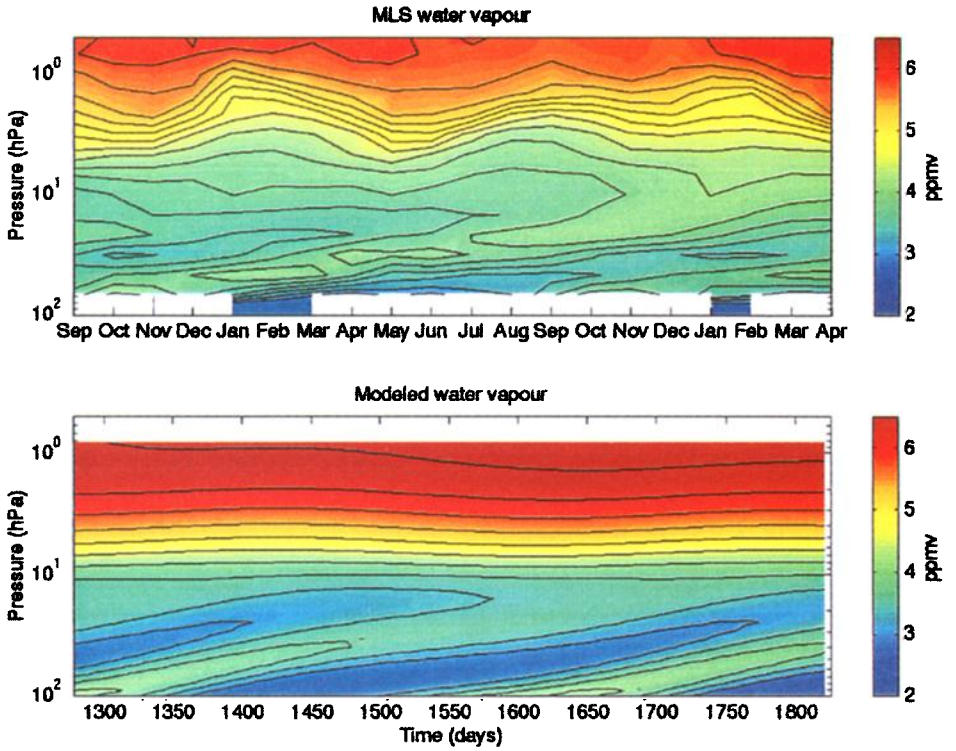

Plate 1. (top) Tropical water vapor measurements from the MLS instrument 1991-1993. (bottom) Water vapor simulated by the 1-D model during 3 years that correspond to the MLS measurements.

the model domain. No specific values or restrictions are given.

4. H_2O Results

The model simulates the long-lived compounds, for example, the main isotope of water vapor and methane, with rather good results. In Figure 1 the vertical profiles of water vapor and methane are plotted. The left panel shows the simulated water vapor (for April) together with H_2O measured in the tropics (-10° to 10°) in April 1993 by HALOE and MLS, both instruments on the UARS satellite (*Lahoz et al.* [1996] (MLS) and *Harries et al.* [1996] (HALOE)). The right panel shows methane from the model and from the HALOE instrument for the same month and latitude. We see that the model slightly overestimates the water vapor and underestimates the methane in the upper levels. In the lower part of the stratosphere on the other hand, the transport seems to be a bit too strong. In this region the methane oxidation is weak due to the very low amounts of OH and $O(^1D)$. The oxidation of methane does not become important until around 20-30 hPa (a little lower in the measurements). The chemistry in the lower part of the stratosphere is sensitive to what time of day we choose for our simulations. At noon there will a lot more production of OH and $O(^1D)$ at low altitudes, and the methane oxidation starts at a lower altitude. The simulation shown in Figure 1 is for 16.00 hours in order to simulate a solar zenith angle of 60°.

The seasonal variation in the input of water vapor causes the wave pattern visible in Figure 1 (left panel). The amplitude of the wave decreases since the vertical diffusion increases with altitude, and above 10 hPa the wave is gone. Plate 1 show a comparison of the modeled H_2O (bottom panel) with tropical MLS data from 1991 to 1993 (top panel). The two agree very well even though the model, again, shows higher values of water vapor than the measurement at the highest levels. Another difference between the two is that the wave pattern is somewhat exaggerated in the model (also seen in Figure 1). This is probably due to mixing of air with the subtropics through the subtropical barriers. The tropical region is not completely isolated, and such mixing is not included in the model.

5. Isotopic Ratio Results

We do not present here any profiles of HDO itself but rather of the isotopic ratio. This is a measure of how well we simulate HDO if the H_2O profiles are realistic. In the first simulation we set the isotopic ratio at the tropopause to a constant value (no annual variation), $\delta D = -580‰$. In Figure 2 the vertical profile of the resulting isotopic ratio is displayed as the thick solid line. The expected decrease of the depletion with altitude, caused by the production of water from methane, shows up clearly. The delta value increases from $\delta D = -580‰$ (prescribed) at the tropopause level to about $\delta D = -360‰$ at 50 km. The increase is slow at

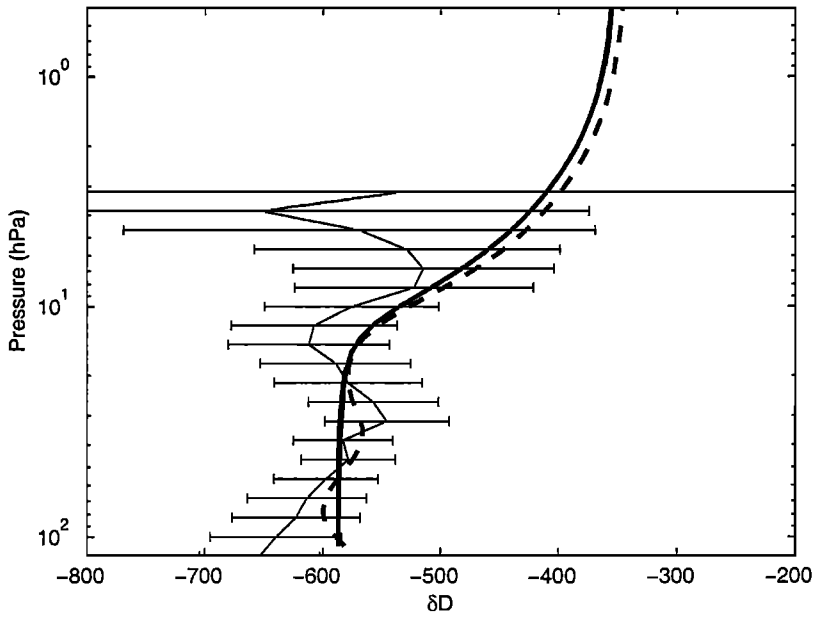

Figure 2. Thick lines are the simulated δD ratio from the tropopause at 100 hPa to 1 hPa. The solid line is with a constant isotopic ratio at the lower boundary, and the dashed line is an input ratio with an annual cycle. The thin solid line shows a measurement by the ATMOS instrument from the tropical region in November 1994. Error bars indicate 1σ levels.

the lower layers since the oxidation of methane is slow in this region.

If we allow the isotopic ratio to vary at the tropopause with an amplitude of 30‰, we see a wave transported upward through the stratosphere (dashed line in Figure 2). The annual cycle produces a wave pattern in the isotopic ratio very similar to the "tape recorder effect" [*Mote et al.*, 1995]. In this case we assume that the largest depletion occurs at the tropopause during northern winter, and the depletion during summer is less severe. Further discussion about the effect of this variation and its strength is found in section 6.2.

There are only a few existing measurements of the isotopic ratio in the stratosphere [e.g., *Dinelli et al.*, 1997; *Rinsland et al.*, 1984; *Abbas et al.*, 1987]. Most of the profiles show that there is a general increase in δD from about -500‰ to -600‰ at 80 hPa to between -400‰ and -300‰ at 2-4 hPa. A wave pattern can be detected but the uncertainties are rather large. One example of a δD profile is shown as the thin solid line in Figure 2. This profile is measured in early November 1994 in the tropics (-20° to 20°) by the ATMOS instrument on the ATLAS-3 shuttle mission [*Gunson et al.*, 1996; *Irion et al.*, 1996]. The figure shows that there is a good agreement between the measurement and the modeled profile (also for November). There is also a clear wave pattern in the measurement that fits well with the model.

These results, both the model and the measurements, show that the isotopic ratio will not fully reflect the isotopic ratio of methane at 1 hPa. The reason for this is that the D/H ratio here will still be influenced by the tropospheric H_2O.

6. Discussion

The isotopic ratio in the model increases with altitude from between δD=-500‰ and -600‰ at the tropopause up to around -300‰ at 1 hPa. This is what we expect according to theoretical assumptions. The few observations that exists also show isotopic ratios similar to this.

Even though the model gives realistic results there are several unsolved questions that can affect the profiles of the isotopic compounds and the resulting isotopic ratio of water vapor. We will discuss a few of them here and try to determine how large their effects are.

6.1. Reaction Rates

In the major reactions, in which CH_3D reacts with OH, $O(^1D)$, and Cl (reactions (R_2), (R_3), and (R_{11})), there are two different branches: one where the D atom moves away from the carbon to form HDO and one where it stays and H_2O is formed. These possibilities have thus far been assumed equally possible. *Irion et al.* [1996] found from measurements that the reaction CH_3D + OH is about 20% slower than the corresponding unsubstituted reaction. One might therefore suspect, that the reaction branch forming HDO is less than the statistical value of one fourth of the total rate. We performed three simulations where we assumed three different branching ratios. In the first case we assume one fourth of the rate constant, i.e., one chance in four that we form HDO (reference case, see above). Then we assume one fifth and, finally, one tenth of the rate constant which would only yield a small amount of HDO in the first step of the oxidation chain. We found that the difference between these three cases was less than

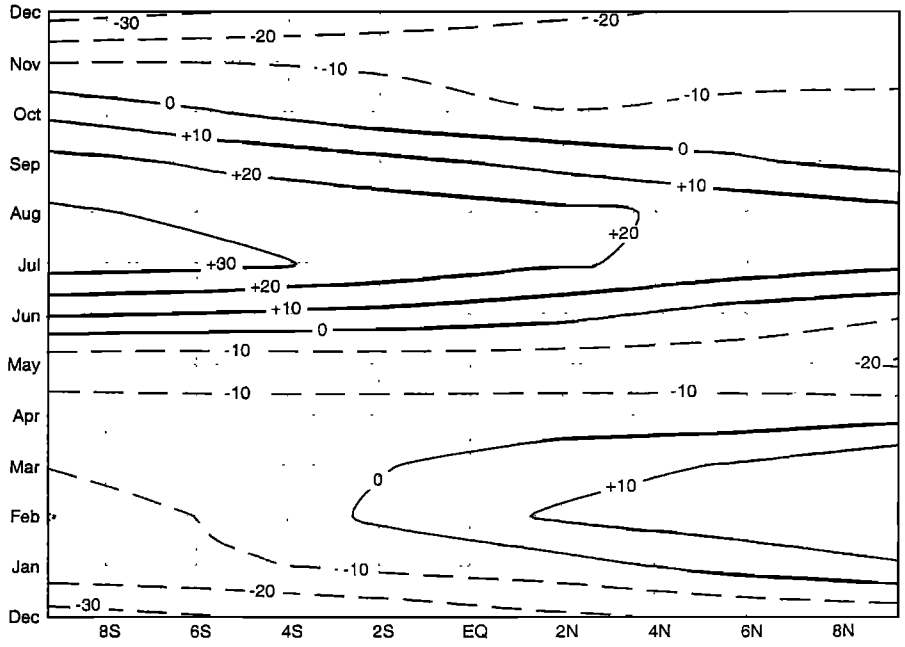

Figure 3. Simulated monthly δD anomalies (mean over all longitudes) near the tropical tropopause, as derived from an ECHAM-4 AGCM simulation. The December values are shown twice for reasons of clarity.

10‰. The small difference is probably because the CH_2D, which remains if H_2O is the product, will continue in the oxidation chain and finally result in a HDO molecule.

We therefore decreased all of the reaction rates for the isotopic reactions given above by 10%. This means that all reactions are slower in the same way as $CH_3D + OH$. The resulting profile did not show any major difference compared to the reference profile either. The δD value at 50 km changed from -360‰ to -370‰.

6.2. Input Ratio

The isotopic ratio at the top of the troposphere and how much of it is injected (through the tropopause "cold trap") is another big uncertainty. It is not only the absolute value that is uncertain but also if there is an annual cycle in the input isotopic ratio, and how large its amplitude would be.

It is very likely that the input ratio will vary throughout the year. Since the isotopic fractionation is temperature dependent (see section 2), it is very probable that the tropopause temperature will affect the isotopic ratio in the lowest part of the tropical stratosphere. The tropopause temperature is lowest during northern winter, and the depletion would therefore be most severe during this season. One reason for the very low temperatures is the strong convection during the same season. The isotopic fractionation due to the vapor pressure effect during condensation is thus expected to be very strong as well. On the other hand, it may also suggest that the "ice lofting" is strongest at the same time. This would, in that case, imply that the isotopic ratio would be less depleted during northern winter. During the northern summer season the convection is less strong, but on the other hand, more widely spread over larger areas (during winter it is mainly over Indonesia). This may cause a larger "net depletion" which enters the stratosphere.

For a first estimate of the annual cycle of HDO in the tropopause region we have studied results of a three-dimensional (3-D) atmosphere general circulation model (AGCM). AGCMs, which explicitly include stable water isotopes in their hydrological cycle, have been developed during the last 15 years. They are capable of simulating many characteristics of the isotopic signature of tropospheric water in vapor, liquid, and solid phase [e.g., *Joussaume et al.*, 1984; *Koster et al.*, 1988; *Hoffmann et al.*, 1998]. Here we refer to results of a simulation using the Hamburg AGCM ECHAM-4 [*Roeckner et al.*, 1996] with both $H_2{}^{18}O$ and HDO included in the water cycle [*Hoffmann et al.*, 1998]. The AGCM was especially adapted to simulate the climate of the middle atmosphere [*Manzini and Bengtsson*, 1996] and a steady state simulation over a period of 1 year was performed in T30 mode (horizontal grid size approximately 3.75° × 3.75°).

In the tropical region between 8°N and 8°S, mean simulated annual δD values near the tropopause were in the range of -720‰ to -800‰. Thus the ECHAM-4 model simulates a stronger depletion of HDO in water vapor than observed in short-time measurements (-500‰ to -600‰; see Figure 2). The discrepancy of the model might be explained by an underestimation of the "ice lofting" effect in convective updrafts, which has already been discussed in section 2.

In Figure 3, the simulated monthly δD anomalies (i.e. monthly deviations from the annual mean value)

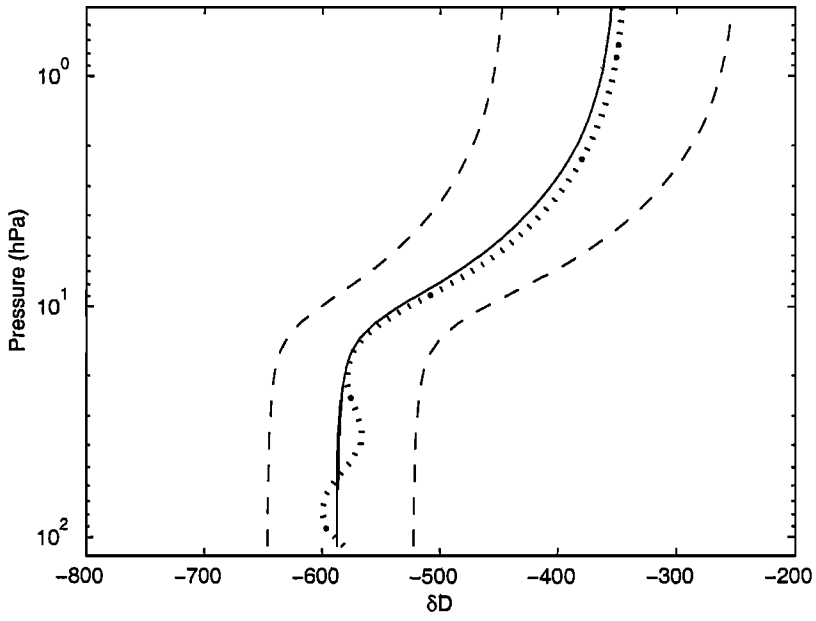

Figure 4. Modeled δD profile with a constant input ratio (solid line) and with an annual cycle (dotted line). Dashed lines are simulated error intervals assuming a 5% error in the H_2O and a 10% error in the HDO profiles.

in the tropical tropopause region are plotted. For the Southern Hemisphere, a clear annual cycle is detected in the simulation results: maximum summer δD values are more than 30‰ higher than the annual average, and minimum winter δD values are about 30‰ lower. For the Northern Hemisphere, a similar but weaker annual cycle is seen. The annual cycles of both hemispheres merge in the equatorial region and because of their asymmetric strength there exists an annual cycle with two maxima and two minima. Hence the ECHAM-4 simulation results indicate an annual δD amplitude of 60‰ and 40‰ at 8°S and 8°N, respectively. However, the reader should keep in mind that the deviations between simulated annual δD values and observations are greater than the simulated amplitude of the annual δD cycle. A better agreement between mean model results and observations (e.g., by an enhanced simulated "ice lofting" effect) might also significantly change the strength of the simulated annual cycle. Thus these AGCM findings should be interpreted with caution and only as a first attempt to estimate the strength of the annual δD cycle in the tropical tropopause region. Both improved 3-D modeling efforts and long-time measurements are needed for a better estimate of the isotopic signature of water vapor near the tropopause.

A few model runs with the 1-D model were made to simulate different scenarios and to see how much the entry isotopic ratio affects the vertical profile. First, we made a simulation where we decreased the entry ratio to −450‰ instead of −580‰ used in the reference case. No annual variation was included in this case. The resulting effect is rather large. The delta value at 1 hPa is about −290‰ instead of −360‰. A change in δD of 130‰ at the lowest layer will thus cause a change in δD of ~70‰ at the highest layer.

If an annual cycle in the input ratio is included the δD value at the highest layers does not change. The vertical diffusion smears out the wave pattern that is caused by the varying isotopic ratio. Depending on which season the isotopic ratio is lowest the "tape recorder wave" will change phase. Apart from this, the different seasons are similar. The amplitude of the input variation causes the wave to extend higher or lower in altitude.

6.3. Effect of Retrieval Errors

The model described in this paper was originally constructed as part of the preparatory work for Odin [*Murtagh et al.*, 2001]. Odin is a small satellite that was launched February 20, 2001. It will be able to measure water vapor and its isotopes. The measurements will, of course, be contaminated with noise. The question is then how much an error in the measured H_2O and HDO profiles will affect the isotopic ratio profile.

To investigate this, we assume that we can retrieve the HDO profile from a measurement, for example, by the Odin satellite, within 10% of the true value. At the same time, H_2O is retrieved within 5%. These precisions will probably be difficult to obtain for single profile retrievals. By using zonal averages however, we can increase the signal to noise ratio considerably. The "error intervals" we obtain for the δD signal are indicated in Figure 4. It is obvious that the wave pattern in the vertical profile, superimposed as the dotted line, cannot be resolved unless the amplitude is larger than 50-70‰.

We would thus need to retrieve the water vapor and deuterium profiles better than assumed here. Retrievals

using simulated Odin spectra show that it may be possible to retrieve HDO better than 10% in the altitude range of 2-70 hPa if zonal mean profiles are created.

6.4. Future Work

The model presented here is a first attempt to model the chemistry and transport of $H_2{}^{16}O$ and HDO. The model needs to be validated in a more rigorous way than the qualitative comparisons made here. Apart from the water vapor we also need to consider the modeled methane and its isotopic ratio. That ratio is particularly interesting since it, to a very large degree, determines the isotopic ratio of water vapor in the upper stratosphere.

Another improvement to the model would be a better description of the tropopause and its role in determining the amount of water vapor entering the stratosphere and the input isotopic ratio. Both the altitude of the tropopause and its temperature need to be considered in the studies of troposphere to stratosphere exchange.

We would also like to include $H_2{}^{18}O$ and its chemistry in the model. This is probably a more difficult task compared to HDO, since there are more compounds containing ^{18}O than D involved in the methane oxidation chain. This also requires investigation and better knowledge about the isotopic ratio of the oxygen compounds involved in order to obtain the correct production of $H_2{}^{18}O$.

Finally, the inclusion of the present chemistry in a more sophisticated, 2-D or 3-D model, is a future goal. This would make it possible to study the isotopic ratio in the midlatitudes and how (or if) it changes with latitude.

Acknowledgments. This work has been supported by grants from the Swedish National Space Board as part of the Odin program. Computing facilities for the ECHAM-4 simulation were provided by the Max Planck Institute of Meteorology and the German Climate Computing Centre (DKRZ) in Hamburg.

References

Abbas, M. M., J. Guo, B. Carli, F. Mencaraglia, A. Bonetti, M. Carlotti, and I. G. Nolt, Stratospheric O_3, H_2O, and HDO distributions from balloon-based far-infrared observations, *J. Geophys. Res., 92,* 8354-8364, 1987.

Brasseur, G., and S. Solomon, *Aeronomy of the Middle Atmosphere,* D. Reidel, Norwell, Mass., 1984.

Brühl, C., and P. J. Crutzen, Scenarios and possible changes in atmospheric temperatures and ozone concentrations due to man's activities, estimated with a one-dimensional coupled photochemical climate model, *Clim. Dyn., 2,* 170-203, 1988.

Craig, H., Standard for reporting concentrations of deuterium and oxygen-18 in natural waters, *Science, 133,* 1833-1834, 1961.

Dansgaard, W., Stable isotopes in precipitation, *Tellus, 16,* 436-438, 1964.

de Grandpre, J., J. W. Sandilands, J. C. McConnell, S. R. Beagley, P. C. Croteau, and M. Y. Danlin, Canadian middle atmosphere model: Preliminary results from the chemical transport module, *Atmos. Ocean, 35,* 385-431, 1997.

DeMore, W. B., S. P. Sander, D. M. Golden, R. F. Hampson, M. J. Kurylo, C. J. Howard, A. R. Ravishankara, C. E. Kolb, and M. J. Molina, Chemical kinetics and photochemical data for use in stratospheric modeling, *JPL Publ. 97-4,* Pasadena, Jet Propul. Lab., Calif., 1997.

Dinelli, B. M., G. Lepri, M. Carlotti, B. Carli, F. Mencaraglia, M. Ridolfi, I. G. Nolt, and P. A. R. Ade, Measurement of the isotopic ratio distribution of $HD^{16}O$ and $H_2{}^{16}O$ in the 20-38 km altitude range from far-infrared spectra, *Geophys. Res. Lett., 24,* 2003-2006, 1997.

Ehhalt, D. H., Vertical profiles of HTO, HDO and H_2O in the troposphere, *Tech. Note TN/STR 100,* Natl. Cent. for Atmos. Res., Boulder, Colo., 1974.

Grooss, J.-U., Modelling of stratospheric chemistry based on HALOE/UARS satellite data, Ph.D. thesis, 135 pp., Johannes Gutenberg-Univ., Mainz, Germany, 1996.

Gunson, M. R., et al., The Atmospheric Trace Molecule Spectroscopy (ATMOS) experiment: Deployment on the ATLAS space shuttle missions, *Geophys. Res. Lett., 23,* 2333-2336, 1996.

Hagemann, R., G. Nief, and E. Roth, Absolute isotopic scale for deuterium analysis of natural waters, Absolute D/H ratio for SMOW, *Tellus, 22,* 712-715, 1970.

Harries, J. E., J. M. Russel III, A. F. Tuck, L. L. Gordley, P. Purcell, K. Stone, R. M. Bevilacqua, M. Gunson, G. Nedoluha, and W. A. Traub, Validation of measurements of water vapor from the Halogen Occultation Experiment (HALOE), *J. Geophys. Res., 101,* 10,205-10,216, 1996.

Hoffmann, G., M. Werner, and M. Heimann, The water isotope module of the ECHAM atmospheric general circulation model: A study on time scales from days to several years, *J. Geophys. Res., 103,* 16,871-16,896, 1998.

Holton, J. R., Troposphere-stratosphere exchange of trace constituents: The water vapor puzzle, in *Dynamics of the Middle Atmosphere,* edited by J. R. Holton and T. Matsuno, pp. 369-385, D. Reidel, Norwell, Mass., 1984.

Holton, J. R., P. H. Haynes, M. E. McIntyre, A. R. Douglass, R. B. Rood, and L. Pfister, Stratosphere-troposphere exchange, *Rev. Geophys., 33,* 403-439, 1995.

Irion, F. W., et al., Stratospheric observations of CH_3D and HDO from ATMOS infrared solar spectra: Enrichments of deuterium in methane and implications for HD, *Geophys. Res. Lett., 23,* 2381-2384, 1996.

Jancso, G., and W. A. van Hook, Condensed phase isotope effects (especially vapor pressure isotope effects), *Chem. Rev., 74,* 689-750, 1974.

Joussaume, J., R. Sadourny, and J. Jouzel, A general circulation model of water isotope cycles in the atmosphere, *Nature, 311,* 24-29, 1984.

Kaye, J. A., Mechanisms and observations for isotope fractionation of molecular species in planetary atmospheres, *Rev. Geophys., 25,* 1609-1658, 1987.

Kaye, J. A., Analysis of the origins and implications of the ^{18}O content of stratospheric water vapor, *J. Atmos. Chem., 10,* 39-57, 1990.

Koster, R.D., P.S. Eagleson, and W.S. Broecker, *Tracer Water Transport and Subgrid Precipitation Variation Within Atmospheric General Circulation Models,* Dep. of Civ. Eng., MIT, Cambridge, Mass., 1988.

Lahoz, W. A., et al., Validation of UARS Microwave Limb Sounder 183 GHz H_2O measurements, *J. Geophys. Res., 101,* 10,129-10,150, 1996.

Le Texier, H., S. Solomon, and R. R. Garcia, The role of molecular hydrogen and methane oxidation in the water vapor budget of the stratosphere, *Q. J. R. Meteorol. Soc., 114,* 281-295, 1988.

Manzini, E., and L. Bengtsson, Stratospheric climate and variability from a general circulation model and observations, *Clim. Dyn., 12,* 615-639, 1996.

McIntyre, M. E., and T. N. Palmer, The "surf zone" in the stratosphere, *J. Atmos. Terr. Phys., 46,* 825-849, 1984.

Merlivat, L., and J. Jouzel, Global climatic interpretation of the deuterium-oxygen 18 relationship for precipitation, *J. Geophys. Res., 84,* 5029-5033, 1979.

Mote, P. W., K. H. Rosenlof, J. R. Holton, R. S. Harwood, and J. W. Waters, Seasonal variations of water vapor in the tropical lower stratosphere, *Geophys. Res. Lett., 22,* 1093-1096, 1995.

Mote, P. W., K. H. Rosenlof, M. E. McIntyre, E. S. Carr, J. C. Gille, J. R. Holton, J. S. Kinnersley, H. C. Pumphrey, J. M. Russel III, and J. W. Waters, An atmospheric tape recorder: The imprint tropopause temperatures on stratospheric water vapor, *J. Geophys. Res., 101,* 3989-4006, 1996.

Moyer, E. J., F. W. Irion, Y. L. Yung, and M. R. Gunson, ATMOS stratospheric deuterated water and implications for troposphere-stratosphere transport, *Geophys. Res. Lett., 23,* 2385-2388, 1996.

Murtagh, D. P., et al., An overview of the Odin atmospheric mission, *Can. J. Phys.,* in press, 2001.

Owens, A. J., C. H. Hales, D. L. Filkin, C. Miller, J. M. Steed, and J. P. Jesson, A coupled one-dimensional radiative-convective, chemistry-transport model of the atmosphere, 1. Model structure and steady state perturbation calculations, *J. Geophys. Res., 90,* 2283-2311, 1985.

Rinsland, C. P., et al., Simultaneous stratospheric measurements of H_2O, HDO and CH_4 from balloon borne and aircraft infrared solar absorption spectra and tunable diode laser laboratory spectra of HDO, *J. Geophys. Res., 89,* 7259-7266, 1984.

Rinsland, C. P., M. R. Gunson, J. C. Foster, R. A. Toth, C. B. Farmer, and R. Zander, Stratospheric profiles of heavy water vapor isotopes and CH_3D from analysis of the ATMOS Spacelab 3 infrared solar spectra, *J. Geophys. Res., 96,* 1057-1068, 1991.

Roeckner, E., et al., *The Atmospheric General Circulation Model ECHAM-4: Model Description and Simulation of Present-Day Climate,* Max Planck Inst. for Meteorol., Hamburg, Germany, 1996.

Shampine, L. F., and M. W. Reichelt, The MATLAB ODE Suite, SIAM, *J. Sci. Comput., 18,* 1997.

Smith, R. B., Deuterium in North Atlantic storm tops, *J. Atmos. Sci., 49,* 2041-2057, 1992.

A. Jonsson, D. P. Murtagh, M. Ridal and M. Werner, Department of Meteorology, Svante Arrhenius v.12, Stockholm University, SE-106 91 Stockholm, Sweden. (email: martin@misu.su.se; andreas@misu.su.se; werner@misu.su.se; donal@misu.su.se)

(Received December 15, 2000; revised May 10, 2001; accepted May 25, 2001.)